Reactive transport of [85]Sr in a chernobyl sand column: static and dynamic experiments and modeling

Stéphanie Szenknect[a,*], Christophe Ardois[a],
Jean-Paul Gaudet[b,*], Véronique Barthès[c]

[a]*Laboratoire d'Etude des Transferts dans les Sols et le sous-sol, IRSN/DEI/SARG, BP n°17,
92262 Fontenay aux Roses Cedex, France*
[b]*Laboratoire d'étude des Transferts en Hydrologie et Environnement, CNRS/INPG/IRD/UJF-UMR 5564,
BP n°53, 38041 Grenoble Cedex 9, France*
[c]*Section d'Application des Traceurs, CEA/DRT/DTEN, 17 rue des Martyrs, 38054 Grenoble Cedex 9, France*

Abstract

The effects of nonlinear sorption and competition with major cations present in the soil solution on radioactive strontium transport in an eolian sand were examined. Three laboratory techniques were used to identify and quantify the chemical and hydrodynamic processes involved in strontium transport: batch experiments, stirred flow-through reactor experiments and saturated laboratory columns. The major goal was to compare the results obtained under static and dynamic conditions and to describe in a deterministic manner the predominant processes involved in radioactive strontium transport in such systems. Experiments under dynamic conditions, namely flow-through reactor and column experiments, were in very good agreement even though the solid/liquid ratio was very different. The experimental data obtained from the flow-through reactor study pointed to a nonlinear, instantaneous and reversible sorption process. Miscible displacement experiments were conducted to demonstrate the competition between stable and radioactive strontium and to quantify its effect on the [85]Sr retardation factor. The results were modeled using the PHREEQC computer code. A suitable cation-exchange model was used to describe the solute/soil reaction. The model successfully described the results of the entire set of miscible displacement experiments using the

---

* Corresponding authors. Fax: +33 4 38 78 51 34.

E-mail addresses: szenknect@chart2.cea.fr (S. Szenknect), gaudet@hmg.inpg.fr (J.-P. Gaudet).

same set of parameter values for the reaction calculations. The column study revealed that the stable Sr aqueous concentration was the most sensitive variable of the model, and that the initial state of the sand/solution system had also to be controlled to explain and describe the measured retardation factor of radioactive strontium. From these observations, propositions can be made to explain the discrepancies observed between some data obtained from static (batches) and dynamic (reactor and column) experiments. Desorbed antecedent species (stable Sr) are removed from the column or reactor in the flow system but continue to compete for sorption sites in the batch system. Batch experiments are simple and fast, and provide a very useful means of multiplying data. However, interpretation becomes difficult when different species compete for sorption sites in the soil/solution system. A combination of batches, flow-through reactor and column experiments, coupled with hydrogeochemical modeling, would seem to offer a very powerful tool for identifying and quantifying the predominant processes on a cubic decimeter scale (dm^3) and for providing a range of radioactive strontium retardation factor as a function of the geochemistry of the soil/solution system.

1. Introduction

In 1987, a site located 2.5 km south west of Chernobyl Nuclear Power Plant was earmarked for the interim storage of surface soil and contaminated tree trunks following the nuclear accident the year before. These materials can be found in trenches a few meters deep. In 1999, one of these trenches (T22) was chosen for carrying out experiments to validate basic models representing radionuclide transfer to soils and aquifers. Trench T22 and the top layer contain fuel particles that dissolve and release ^{90}Sr. For 15 years, strontium has been penetrating the unsaturated soil zone and the water table with the result that ^{90}Sr activity in the water table varies between 10 and 13 000 Bq/L, while the plume can be seen to spread over a few tens of meters downstream of trench T22 (Bugaï et al., 2002; Dewiere et al., 2004).

Radionuclide mass (activity) transfer to the aquifer is controlled by the fuel particle mass (activity) available for the dissolution process, fuel dissolution mechanisms, waste material sorption parameters, sorption parameters and structure of the surrounding undisturbed, unsaturated soil layer, and the water inflow rate from the surface. The activity distribution in the waste burial site is very heterogeneous, as indicated by in situ trench characterization data based on indirect measurements (Dewiere et al., 2004). Prediction of contaminant transport in the subsurface is strongly influenced by the hydraulic and chemical properties of the soil, processes such as advective and diffusive transport, hydrodynamic dispersion, adsorption and desorption, as well as biological and chemical transformations (Brusseau, 1994; Fesch et al., 1998; Gabriel et al., 1998; Albrecht et al., 2003). Variability in the hydraulic and chemical properties of the soil can cause large spatial differences in rates of contaminant transport from the surface to the groundwater. This, together with the fact that water and radionuclides are unevenly distributed over the Pilot Site in spatial and temporal terms, has caused contaminants (^{90}Sr) to arrive at depths at varying times. In many cases, chemical effects can be far more significant than

hydraulic effects in explaining the differences in arrival times (Thomasson and Wierenga, 2003).

A number of solute transport models covering many of the hydraulic and chemical processes affecting transport through the subsurface already exist (for a recent review, see Šimùnek et al., 2003). Use of these models on a field scale requires knowledge of many parameters used for describing underlying physical and chemical processes (Pang and Close, 1999). The lack of parameter values, the recognized uncertainty relating to field-scale mechanisms responsible for solute movement in natural soils, and the questionable representativeness of samples (Jury and Sposito, 1985) make it very difficult to use comprehensive models for field-scale studies. We therefore opted to use a simplified model for solute transport through the subsurface, assuming that the convective–dispersive transport equation, where chemical interactions are represented by a range of retardation factors (R), can successfully be used to make field-scale predictions of ^{90}Sr transport through the unsaturated zone and in the aquifer. In order to gain insight into the impact of various chemical mechanisms and processes on strontium arrival time and to define as narrow a range of retardation factors as possible, it was decided to perform experiments on the laboratory scale under closely controlled initial and boundary conditions and to use a comprehensive model on this reduced scale.

This work examined the effect of nonlinear sorption and competition with major cations present in the soil solution, on radioactive strontium transport in the eolian sand of the Chernobyl Pilot Site (CPS). Three main laboratory techniques were used to identify and quantify the chemical processes involved in strontium transport. Batch experiments were performed to study the chemical equilibrium state of the soil/solution system under static conditions. Stirred flow-through reactor experiments were conducted to study the kinetics and reversibility of the sorption reaction of strontium at the surface of solid particles under dynamic conditions. Lastly, the transport of strontium was studied in the structured porous medium under saturated flow conditions in laboratory columns. The aim of the study was also to compare the results obtained under static and dynamic conditions, (Bajracharya et al., 1996; Fesch et al., 1998; Porro et al., 2000; Plassard et al., 2000; Tran et al., 2002), but focusing on the initial physical and chemical conditions in the soil/solution system.

2. Materials and methods

2.1. Study site and soil characterization

The near-surface geological column of the CPS consists of the following layers (Dewiere et al., 2004): an artificial topsoil layer (~114.5–114 m a.s.l.), eolian sand (~114–109.5 m a.s.l.), and alluvial sandy sediments (109.5–104 m a.s.l.). The depth to ground water table is 2–3 m. The annual infiltration recharge to groundwater table ranging from 200 to 250 mm/year (30–40% of the yearly precipitation). The hydraulic conductivity of eolian sands is estimated to be 3–5 m/day. For 15 years following waste disposal, ^{90}Sr has been leached from the T22 and has been penetrating the unsaturated zone and the eolian sand aquifer.

The soil used for this study comes from Pripyat Zaton exposure, located 2 km north-east of the CPS. The geological characterization of the Pilot Site and its geological analog, Pripyat Zaton, demonstrated the continuity of the sedimentary suites on a regional scale (Bugaï et al., 2000). Sand from Pripyat Zaton was not contaminated with ^{90}Sr. Hence, it was possible to sample sediments directly from the wall (~2-m high×10-m long) of the exposure and to bring them back to the laboratory. Samples were collected on a grid, then mixed to obtained an average sample of 20 kg. The typical soil bulk density (ρ_d) is 1.7 g/cm^3 and the porosity (ε) is 35%.

The soil sample was dry sieved and the <1 mm fraction used for characterization and laboratory experiments (the >1 mm fraction represented less than 1% of the total sample mass). Soil particle size distribution (Fig. 1) was determined using a laser granulometer (Beckam-Coulter LS230, NF ISO 13320-1). The main components of the soil were determined by chemical and X-ray diffraction analyses. The mineralogical composition of the sand by percentage mass was: 95–98% quartz and <5% feldspar. The X-ray diffraction analysis of the isolated fine fraction revealed the presence of illite and kaolinite. The chemical composition of the sand by percentage abundance was: 95–98% SiO_2, <2% $Al_2O_3+Fe_2O_3$ (measured by ICP-AES after acid digestion). The cation exchange capacity (CEC) of the soil determined using the sodium acetate saturation method (Metson, 1956) is 1.25 meq/100 g, organic carbon content measured by wet combustion is <0.3%, and specific surface area measured by N_2 adsorption using the BET model (Beckam-Coulter SA3100) is 1–2 m^2/g. Sand particle density was assumed to be equal to that of quartz, i.e., 2.65 g/cm^3 (Bolz and Tuve, 1976, pp. 192).

2.2. Synthetic groundwater and solutes

All column, batch and reactor tests were conducted using synthetic groundwater, formulated to approximate the composition observed in CPS aquifer samples. Chemical compositions of synthetic groundwater and field samples are compared in Table 1. The concentrations of major cations chosen for synthetic water were in the range of field concentrations. The highest concentrations were measured in the wells located down-stream of the trench. These concentrations were not representative of the equilibrium state
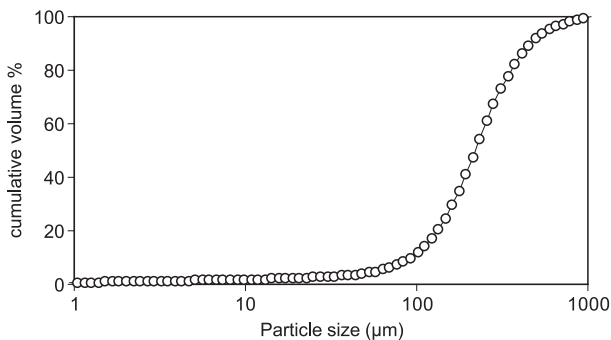
Fig. 1. Cumulative size distribution by volume of studied eolian sand.

Table 1
Comparison of Chernobyl Pilot Site aquifer and synthetic groundwater compositions

Component	Synthetic groundwater	Pilot site aquifer			
	Base chemistry (mol/L)	Average (mol/L)	Standard deviation (mol/L)	Min (mol/L)	Max (mol/L)
Ca^{2+}	$7.7 \times 10^{-5} \pm 1 \times 10^{-5}$	3.56×10^{-4}	4.4×10^{-4}	4.97×10^{-5}	1.98×10^{-3}
K^+	$5.9 \times 10^{-5} \pm 1 \times 10^{-5}$	9.63×10^{-4}	7.5×10^{-5}	2.07×10^{-5}	2.74×10^{-4}
Na^+	$5.7 \times 10^{-5} \pm 1 \times 10^{-5}$	5.21×10^{-5}	6.6×10^{-5}	1.41×10^{-5}	2.21×10^{-4}
Mg^{2+}	$2.1 \times 10^{-5} \pm 0.5 \times 10^{-5}$	4.20×10^{-5}	6.0×10^{-5}	7.5×10^{-6}	1.87×10^{-4}
Sr^{2+}	0	8.4×10^{-6a}	6.9×10^{-6a}	4.9×10^{-6a}	3.71×10^{-5a}
Cl^-	$4.0 \times 10^{-5} \pm 1 \times 10^{-5}$				
SO_4^{2-}	$1.1 \times 10^{-4} \pm 1 \times 10^{-5}$				
Ionic strength	5.72×10^{-4}				
pH	6.4 ± 0.2				

Average concentrations and standard deviations were calculated from 180 samples analyzed by SAA.

[a] Sr^{2+} results were calculated from only 19 samples, as the others were below the detectable level of 4.5×10^{-6} mol/L.

but were disturbed by leaching of the waste contained in the trench. The composition of the water in equilibrium with the eolian sand was determined experimentally. The concentrations of major cations were close to those of the synthetic water. The first conditioning stage of all column and reactor experiments was then reduced.

Synthetic groundwater was prepared by adding cations as sulfate salts to distilled, deionized water, except for K, which was added as chloride, and Ca as carbonate. The pH was adjusted to 6.4 ± 0.2 by adding 0.1 N H_2SO_4. The theoretical concentrations were then verified by chemical analysis with a capillary ion analyzer (Waters).

Known stable strontium concentration solutions were prepared by adding amounts of strontium chloride salt to the previous synthetic groundwater. A wide range of concentrations ranging from 10^{-3} to 10^{-9} mol/L was studied. For radiometric measurements, spiked strontium solutions were also prepared using ^{85}Sr as a radioactive tracer. This isotope was chosen as a tracer because its good gamma-emission of 514 keV and short radioactive half-life of 64.85 days lead to very low concentrations from 10^{-12} to 10^{-8} mol/L in solution.

2.3. Batch experiments

Batch tests were performed at room temperature (22 ± 2 °C) in 16 mL polycarbonate tubes. For all experiments, a solid/solution ratio of 1 g/mL (10 g soil/10 mL solution) was used. The sand was added to the tubes and weighed to the nearest 0.01 g. The required solutions were then added to each tube and brought into contact under mechanical agitation in rototubes for 24 h. Kinetics experiments performed showed that solid/solution equilibrium was reached within this time. Blank experiments with no solid did not reveal any adsorption of chemical species and radioactive tracer on vials. Phase separation was then carried out by temperature-controlled centrifugation at $22\,000 \times g$ for 15 min. Supernatant was then transferred to each tube and the weight checked for subsequent radiochemical analyses.

In order to obtain the strontium adsorption isotherm, the total concentration of strontium adsorbed onto the solid and the remaining concentration in solution at equilibrium must be calculated. These concentrations can be determined through the use of the radioactive tracer. The concentrations were calculated as follows: the aqueous strontium concentration was defined as the ^{85}Sr activity remaining in the supernatant divided by the initial activity, then multiplied by the initial total strontium concentration. It was assumed that the loss in Sr amount was fixed to the solid and this was used to calculate the adsorbed strontium concentration.

Strontium partitioning between the solid and liquid phase was defined and computed from:

$$[Sr]_s = \frac{V}{M} \left[\frac{A(^{85}Sr)_i}{A(^{85}Sr)_{eq}} - 1 \right] [Sr]_{aq} \tag{1}$$

where $[Sr]_s$ is the amount of total Sr sorbed by the soil (mol/kg), $[Sr]_{aq}$ is the total strontium concentration in equilibrium solution (mol/L), $A(^{85}Sr)_i$ is the initial volumetric activity concentration in the solution (Bq/L), $A(^{85}Sr)_{eq}$ is the remaining volumetric activity concentration of the equilibrium solution (Bq/L), V is the volume of the solution (L) and M is the mass of dry soil in suspension (kg).

2.4. Flow-through reactor experiments

Flow-through reactors were used to study mass transfer kinetics at the solid–liquid interface (van Capellen and Qiu, 1997a,b; Martin-Garin et al., 2003). The flow rate can be varied to see how solution residence time in the reactor affects the reaction rate and to determine the characteristic time of solute sorption and desorption. Comparison of characteristic times is a powerful method for isolating the predominant physical or chemical processes involved in reactive solute transport (Sardin et al., 1991). Break-through experiments were also performed in order to measure the sorption and desorption isotherms of chemical species in the presence of a suspended solid (Grolimund et al., 1995; Martin-Garin et al., 2003).

In a perfectly stirred flow-through reactor, the solution composition is homogeneous in the reactor and equal to that measured in the outlet flow. The theoretical evolution over time of the outlet concentration C_{aq} (mol/L) of an inert species after a stepwise increase in the input concentration from 0 to C_0 is given by (Villermaux, 1985):

$$C_{aq}(t) = C_0 \left[1 - \exp\left(-\frac{t}{\tau}\right) \right] \tag{2}$$

where $\tau = V_r/Q$ (h) is the solution residence time in the reactor, V_r (mL) is the volume of solution contained in the reactor, and Q (mL/h) is the flow rate. The theoretical evolution over time of the outlet concentration C_{aq} (mol/L) of an inert species after a stepwise decrease in the input concentration from C_0 to 0 is given by (Villermaux, 1985):

$$C_{aq}(t) = C_0 \exp\left(-\frac{t}{\tau}\right) \tag{3}$$

For a reactive species, the BTC deviates from that predicted by Eqs. (2) and (3). In the case of Sr^{2+} uptake by suspended particles of sand, the amount of sorbed (respectively desorbed) strontium is given by the difference in surface area between the inert tracer BTC predicted by Eq. (2) (respectively Eq. (3)) and the Sr BTC (see Fig. 2). The reversibility of the sorption reaction can be tested by calculating the strontium mass balance (the amount of desorbed strontium divided by the amount of sorbed strontium).

Fig. 3 represents the stirred flow-through reactor experimental setup. The flow-through reactor had an internal volume (V_r) of 34 ± 0.5 mL determined gravimetrically. A mass of 8 g of sand was added to the tared reactor and weighed to the nearest 0.01 g. The soil suspension in the reactor was continuously stirred by the reactor rotation, thus avoiding the need for a magnetic bar in the reactor. A constant flow rate was supplied by a mechanical piston pump (Pharmacia P-500). Aqueous solution flowed into and out of the reactor through 0.45-μm pore size hydrofoil Teflon membranes (HVLP, Millipore). The experiments were carried out at 22 ± 2 °C. Before each experiment, the reactor was washed with 5% nitric acid solution, then rinsed with distilled, deionized water. The outflow solutions were monitored on-line for pH, conductivity, and radionuclide activity. A beta–gamma flow scintillation analyzer (Packard 500TR Series) was used for on-line radiometric analysis of outflow solutions. The activity of prepared standards was measured frequently so that corrections could be made for any instrument drift and radioactive decay.

Reactor performance was improved by imposing a step change from synthetic groundwater to tritiated synthetic groundwater ($C_0(^3H)$=370 kBq/L). The tritiated water experiments were performed at 100 mL/h with and without sand, and Eqs. (2) and (3) were used to describe the normalized BTC ($C_{aq}/C_0(t)$) of the tritiated water (inert tracer).

Strontium sorption experiments on Pripyat Zaton eolian sand were performed using synthetic groundwater solutions in the following sequence. (Stage I) Synthetic groundwater was pumped through the reactor until soil/Sr-free solution equilibrium was reached. (Stage II) The input was switched to the solution containing Sr with an otherwise identical composition to that of groundwater. Strontium initial concentrations in the feed solutions, $[Sr]_0$, ranged from 4.85×10^{-5} mol/L to $\times 10^{-8}$ mol/L, initial activity of all the solutions
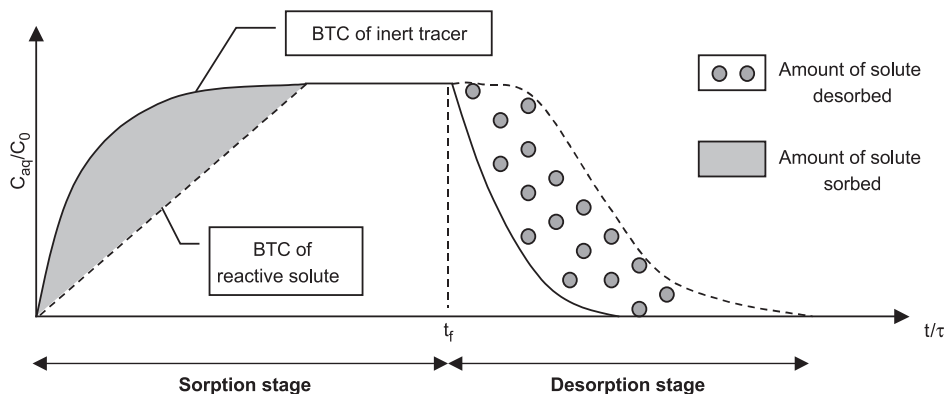
Fig. 2. Typical flow-through reactor BTCs of inert and reactive solutes, and expected results.
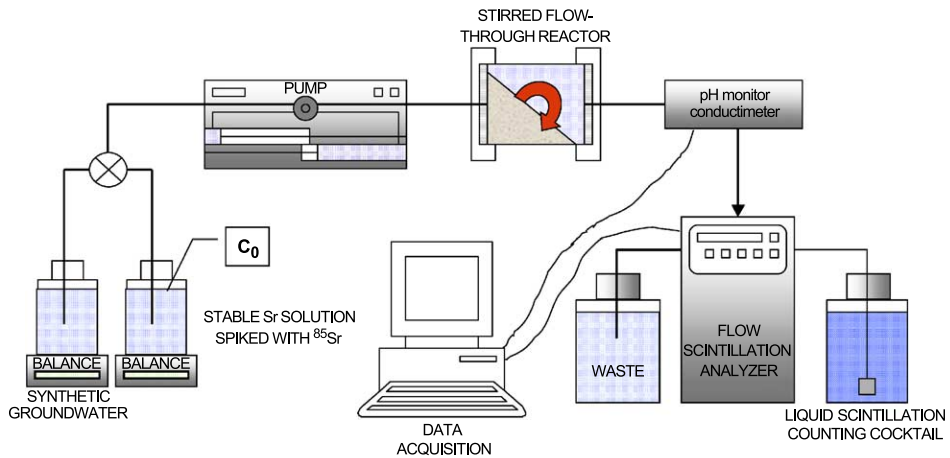
Fig. 3. Stirred flow-through reactor experimental setup.

spiked with [85]Sr was 370 kBq/L. The solution containing Sr was supplied at a constant flow rate until steady state was reached. Once steady state is reached, the total dissolved strontium concentration $[Sr]_{aq}$ remains constant in the outflow. (Stage III) In a number of experiments, strontium desorption was monitored by switching back to synthetic groundwater. Table 2 provides a summary of the experimental conditions of the strontium breakthrough experiments performed.

Blank tests performed with a solution of stable strontium spiked with [85]Sr ($[Sr]_0 = 1.1 \times 10^{-7}$ mol/L) revealed no significant strontium sorption by the reactor materials or filters.

2.5. Column experiments

All column experiments were conducted at 22 ± 2 °C. The experimental setup is shown in Fig. 4. The solutions were fed to a dual-piston pump (Pharmacia P-500). Flow rate was 10 mL/h while the corresponding Darcy's velocity was 5.0 cm/h. The pump

Table 2
Flow-through reactor experiment conditions

Inflow concentration ($[Sr]_0$; mol/L)	Flow rate (Q; mL/h)	Theoretical water residence time (τ; min)	Stage I (t/τ)	Stage II (t/τ)	Stage III (t/τ)	Sr mass balance (%)
4.85×10^{-5}	100	20.4	50	17.1	14.6	80
1.17×10^{-5}	100	20.4	50	11.0	–	–
1.14×10^{-6}	100	20.4	50	21.4	43.2	85
1.1×10^{-7}	100	20.4	50	23.6	35.5	100
1.1×10^{-8}	100	20.4	50	24.4	45.3	100
1.09×10^{-6}	200	10.2	50	29.7	67.8	85
1.09×10^{-6}	20	102	50	29.6	54.7	85

Inflow solutions were stable Sr solutions spiked with [85]Sr. Theoretical water residence time was calculated as the ratio between the gravimetrically measured internal volume of the reactor and flow rate delivered by the piston pump.
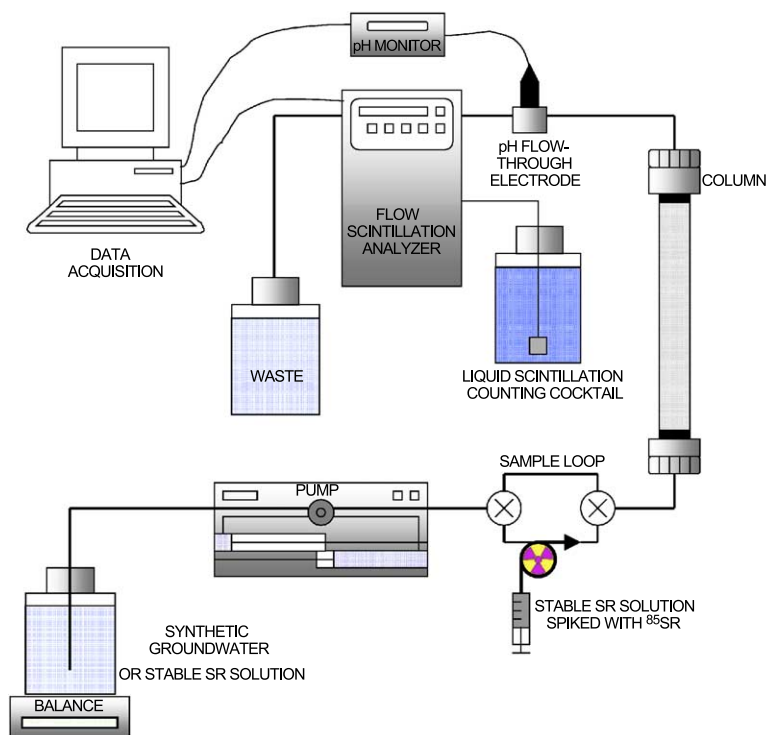
Fig. 4. Experimental setup for miscible displacement experiments.

was connected to the bottom of the column. A Teflon sample loop (500 μL, Rheodyne) linked to a 2×3-way injection valve was coupled up to allow inert and reactive tracer pulse injection. The column outlet was connected to a pH flow cell, and the pH electrode was inserted into the flow cell and connected to the pH monitor (Amersham Pharmacia Biotech). In addition, a beta–gamma flow scintillation analyzer (Packard 500TR Series) was connected to the column outlet to obtain an on-line measurement of the beta or gamma activity outflow.

A glass column (Pharmacia LKB C16, diameter of 16 mm and approximate length of 20 cm) with polypropylene end pieces was equipped with 0.45-μm pore size hydrofoil Teflon membranes (HVLP, Millipore). Teflon 1/16″ capillaries were used to connect the elements. The column was packed dry. The sand bed length was 19.7 cm. Assuming a solid-particle density of 2.65 g/cm^3 and knowing the weight of sand introduced in the column, the bulk density and geometric porosity were calculated (ρ_d=1.75 g/cm^3 and ε=0.34). To minimize gas entrapments, the column was saturated with N$_2$O gas, then slowly saturated (at a flow rate of 1 mL/h) from bottom to top with the feed solution (free-strontium synthetic groundwater or stable strontium solution) with 20 to 140 pore volumes (one pore volume of the column is the fraction of the total volume of the column occupied by water, calculated by $V_p = \theta_{sat} SL$, where θ_{sat} is the saturated water content, S is the section of the column, and L is the length). The

aim of this first stage was to equilibrate the porous medium with the tracer-free solutions. The pulse of tracer-spiked solution composed of identical major ions composition was then injected by switching the injection valve. The pulse was then displaced by the tracer-free solution. BTCs were determined for the nonreactive tracer prior to the strontium experiments. Tritiated synthetic groundwater was used as an inert tracer-spiked solution. The initial activity of tritiated synthetic groundwater was 370 kBq/L. Several inert tracer BTCs were performed during the miscible displacement experiments to ensure that sand-packed column transport properties did not change over time.

Breakthrough curves of the conservative tracer were analyzed using the TableCurve®2D 4.0 (User's manual, SPSS) computer code that uses the analytical solution of the advection–dispersion equation for a Dirac input function (Wen and Fan, 1975). TableCurve uses the Levenburg–Marquardt algorithm for fitting its nonlinear equations and user-defined functions. Eq. (4) is the advection–dispersion equation:

$$\frac{\partial C_{aq}}{\partial t} = -v\frac{\partial C_{aq}}{\partial z} + D\frac{\partial^2 C_{aq}}{\partial z^2} \qquad (4)$$

where C_{aq} (mol/L) is the concentration of conservative (or inert) solute in the outflow.

This made it possible to estimate parameter values of the hydrodynamic dispersion coefficient D (m^2/s, $D=\alpha v+D_e$, where D_e is the effective diffusion coefficient (m^2/s) and α is the dispersivity (m)) and the pore water flow velocity, v (m/s). The water residence time in the column, T_s is calculated as the ratio between the length of the column and the pore water flow velocity ($T_s=L/v$).

For the reactive tracer experiments, different equilibrating solutions were prepared by adding stable Sr as chloride salt to the synthetic groundwater. The concentration of stable strontium in equilibrating solutions was $\leq 10^{-5}$ mol/L. ^{85}Sr was added to the equilibrating solution to prepare the pulse solution and ^{85}Sr BTCs were monitored at the outlet of the column. Table 3 provides a summary of the experimental conditions and results for the different column tests. The mass balance of ^{85}Sr was calculated using the 0-order temporal moment of the BTC. The retardation factor, R, was calculated as the ratio between the first-order moment of the ^{85}Sr BTC, or mean residence time of reactive solute and the water residence time T_s (see Jury and Roth, 1990 or Schoen et al., 1999 for a detailed explanation of the temporal moments method).

Table 3
Column experiment conditions

[Sr]$_{aq}$ in feed solution (mol/L)	Equilibrium stage (V_p)	[Sr]$_{aq}$ in pulse (mol/L)	[^{85}Sr]$_{aq}$ in pulse (mol/L)	^{85}Sr mass balance (%)	Retardation factor ($R=T_s(^{85}$Sr$)/T_s(^3$H$)$)
0	20	0	1.4×10^{-8}	100	242
9.5×10^{-7}	140	9.5×10^{-7}	5×10^{-10}	100	103
2.48×10^{-6}	140	2.48×10^{-6}	1.9×10^{-9}	100	85
8.00×10^{-6}	140	8.00×10^{-6}	1.3×10^{-9}	100	33

Isotopic compositions of equilibrating solution and injected solution are compared.

2.6. Data analysis and modeling

2.6.1. Interaction mechanism

Strontium in solution is assumed to be present mainly in the form of an uncomplexed Sr^{2+} ion. Only in highly alkaline soils could strontianite ($SrCO_3$) control strontium concentration in solutions. The extent to which strontium partitions from the aqueous phase to the solid phase is assumed to be controlled primarily by the CEC of the solid phase and ionic strength of the soil solution (Koss and Kim, 1990; Ohnuki, 1994). It has also been reported that most of the Sr^{2+} in solution is reversibly sorbed onto soil (Jackson and Inch, 1983). These findings are consistent with the cation exchange proposed as the mechanism generally controlling strontium adsorption (Keren and O'Connor, 1983; Lefevre et al., 1993a,b). In media, where pH is greater than 9 and where carbonates predominate, coprecipitation with $CaCO_3$ and precipitation as $SrCO_3$ may become an increasingly significant mechanism in controlling strontium removal from solution (Lefevre et al., 1993a,b). A negative correlation between solution pH and amount of Sr^{2+} sorbed has been reported (Prout, 1958; Keren and O'Connor, 1983; Koss and Kim, 1990). This trend is probably due to protons competing with Sr^{2+} for exchange sites and to the result of pH increasing the CEC. It has been reported that Ca^{2+} exerts a specific depressing effect on Sr^{2+} adsorption. It is true that calcium is found in groundwater at concentrations typically 2 orders of magnitude greater than stable strontium and 12 orders of magnitude greater than radioactive strontium. Moreover, the valence state, the radius of hydrated Ca^{2+}, and the free energy of hydration of suggest that Ca^{2+} has a greater capacity for displacing strontium from an exchange site than other more common groundwater cations (Kinniburgh et al., 1975). Competition between Sr^{2+} and Ca^{2+} for site accessibility is taken into account in strontium interaction modeling through the selectivity coefficient $K_{Sr/Ca}$. As calcium and strontium are similar cations, $K_{Sr/Ca}$ can be expected to be approximately one (Bolt and Bruggenwert, 1978).

The main reactions and processes involved in the laboratory experiments were simulated using the PHREEQC (Version 2) computer program for speciation, batch-reaction and one-dimensional transport. The PHREEQC code has been successfully applied in various geochemical modeling studies (Appelo et al., 1998; van Breukelen et al., 1998; Prommer et al., 1999; Hormann and Kirchner, 2002). A full description of its mathematical background can be found in the program manual (Parkhurst and Appelo, 1999).

PHREEQC solves the set of balance equations for the chemical reactions:

■ Precipitation–dissolution of: $SrCO_3(s)$, $SrSO_4(s)$, $SrCl_2(s)$,
■ Complexation/dissociation of: $SrCl^+$, $SrCl_2$, $SrOH^+$, $SrCO_3$, $SrHCO_3^+$, $SrSO_4$.

Ion exchange equilibria are calculated by PHREEQC using the Gaines and Thomas convention. For a binary reaction involving two cations, A^{a+} and B^{b+}, competing for a soil exchanger X,

$$\frac{1}{a}A^{a+} + \frac{1}{b}B - X_b \leftrightarrow \frac{1}{a}A - X_a + \frac{1}{b}B^{b+} \tag{5}$$

the selectivity coefficient $K_{A/B}$ of A^{a+} for B^{b+} exchange is (according to the Gaines–Thomas convention):

$$K_{A/B} = \frac{(A - X_a)^{1/a} [B^{b+}]^{1/b}}{(B - X_b)^{1/b} [A^{a+}]^{1/a}} \tag{6}$$

where square brackets denote thermodynamic activities in solution and parentheses denote the equivalent cation of exchangeable fraction on the exchanger. It is assumed that the exchange complex is always fully occupied by cations.

In PHREEQC, all cation exchange reactions are related to Na^+, which has been chosen as the reference cation. For example, the reaction given by Eq. (5) is split into two half-reactions as:

$$\frac{1}{a}A^{a+} + Na - X \leftrightarrow \frac{1}{a}A - X_a + Na^+ \tag{7}$$

$$\frac{1}{b}B^{b+} + Na - X \leftrightarrow \frac{1}{b}B - X_b + Na^+ \tag{8}$$

The selectivity coefficient $K_{A/B}$ is then calculated as:

$$K_{A/B} = K_{A/Na}/K_{B/Na} \tag{9}$$

For most of the chemical processes taken into account in the calculations, the thermodynamic constants given in the PHREEQC database were used. The selectivity coefficient with respect to Na^+ of the major cations, K^+, Mg^{2+}, Ca^{2+}, provided by the PHREEQC database were derived from the compilation made by Bruggenwert and Kamphorst (1982). The selectivity coefficient of Sr^{2+} with respect to Na^+ was determined on the basis of the results of this study.

The experiments in this study were modeled by adding a new species to the PHREEQC database in order to distinguish ^{85}Sr, the radioactive isotope of strontium. It was assumed that ^{85}Sr had the same chemical characteristics as stable strontium, meaning that it was involved in the same chemical reactions defined with the same thermodynamic constants as stable strontium. Competition between $^{85}Sr^{2+}$ and stable Sr^{2+} was allowed assuming that $K_{85_{Sr/Sr}}=1$.

2.6.2. Reactive transport model

PHREEQC is capable of modeling a one-dimensional, advection–dispersion transport process. This process can be combined with equilibrium and kinetic chemical reactions. Conservation of mass for a transported chemical yields the following advection–reaction–dispersion equation:

$$\frac{\partial [Sr]_{aq}}{\partial t} = -v \frac{\partial [Sr]_{aq}}{\partial z} + D \frac{\partial^2 [Sr]_{aq}}{\partial z^2} - \frac{\partial q}{\partial t} \tag{10}$$

where $[Sr]_{aq}$ is the total concentration of strontium in solution (mol/L), t is time (s), v is pore water flow velocity (m/s), z is distance (m), D is the hydrodynamic dispersion coefficient (m^2/s), and q is the concentration of strontium sorbed onto the soil (mol/L)

expressed in the same units as $[Sr]_{aq}$ in PHREEQC. In fact, q is calculated as $\rho_d/\varepsilon.[Sr]_s$ where $[Sr]_s$ (mol/kg) is the amount of strontium sorbed per mass of soil. The term $\partial q/\partial t$ is the change in concentration in the solid phase due to the reactions mentioned in the previous section. For a conservative solute, this term is equal to 0 (see Eq. (4)).

The boundary conditions appropriate for laboratory column and reactor experiments with inlet tubing much smaller than inlet cross-section, are flux conditions defined at $z=0$ as:

$$[Sr]_{aq}(0,t) = [Sr]_0 + \alpha \frac{\partial [Sr]_{aq}(0,t)}{\partial z} \tag{11}$$

The initial conditions depend on the experimental methodology. The initial distribution of stable strontium sorbed onto the sand was particularly important and the "history" of the sand bed prior to the tracer injection had to be simulated accurately.

The transport parameters fitted with TableCurve to the BTC of the conservative tracer were used in the PHREEQC input file to simulate the transport of reactive solutes. At this stage, the only parameters fitted were the exchange capacity (in mol/L) and the selectivity coefficient of strontium with respect to Na^+. These two parameters were determined based on the stirred flow-through reactor study, and the validity of the model was then tested in batches under static conditions and in a structured sand column under dynamic conditions.

3. Results

3.1. Batch studies

"Direct" batch experiments were performed for the sand/synthetic water system and the resulting strontium sorption isotherms are shown in Fig. 5. For low stable strontium concentrations at equilibrium ($[Sr]_{aq}<10^{-6}$ mol/L), the isotherm is linear and the corresponding distribution coefficient (Kd) value obtained is 13.5 mL/g. For higher strontium concentrations, strong nonlinear behavior is observed, and the sorption coefficient decreases as the strontium concentration increases. This effect is probably due to the well-known competition effect (Hilton et al., 1997) between Sr^{2+} and major
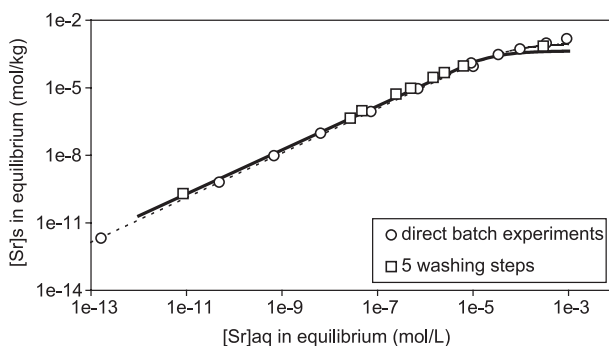
Fig. 5. Strontium sorption isotherms on the eolian sand and related fitted curves using the Langmuir model (○ direct batch experiments and □ five washing steps).

dissolved cations (Ca^{2+}, Mg^{2+}). A Langmuir model described the previous isotherms quite well:

$$[Sr]_s = \frac{KS_{max}}{1 + K[Sr]_{aq}} [Sr]_{aq} \tag{12}$$

where S_{max} is the sorption capacity of the soil (mol/kg) and K (L/mol) is the Langmuir constant. The parameter values fitted to the "direct" batch experiment isotherm are 9.2×10^{-4} mol/kg for S_{max} and 1.45×10^4 L/mol for K.

As the stable Sr^{2+} concentration is one of the main factors controlling sorption of the radioactive strontium tracer, and nonlinear behavior begins at quite low Sr^{2+} concentrations, the initial presence of strontium in the studied sand was checked by bringing the sand into contact with deionized water and synthetic water for 3 days. The composition of water at equilibrium was then measured (Table 4).

For the deionized water/sand system, a slight dissolution of the matrix was observed, together with a final stable strontium concentration of 10^{-6} mol/L. For the synthetic water/ sand system, a lower slightly stable strontium concentration of 3×10^{-7} mol/L was reached. Such concentrations are not far from the critical concentration above which nonlinear behavior is observed. They should therefore be taken into account to calculate the real strontium concentration initially present. Changes in the chemical composition of both solutions were also checked. Using the fresh synthetic water as a reference (Table 1), an increase of K^+ and Ca^{2+} concentrations was observed in the synthetic water/sand system, whereas Na^+ and Mg^{2+} concentrations were close to those observed in the fresh synthetic water. For the deionized water/sand system, a higher K^+ concentration and a lower Na^+ concentration were observed, while the two remaining cations were at the same level as in the fresh synthetic water. These measurements indicate that synthetic water is not in equilibrium with sand, and that the initial chemical composition of water may influence the dissolution and equilibrium of the sand/solution system.

A second type of batch experiment was performed to study the impact of the initial equilibrium state of the solution/sand system on the actual sorption isotherm of strontium. Sand was first brought into contact for 24 h with synthetic water without stable strontium and radioactive tracer. After phase separation by centrifugation, supernatant was carefully removed and replaced by fresh synthetic water. This washing step was repeated four times to equilibrate the solid/solution system. The strontium sorption isotherm was then determined according to the procedure used for "direct" batch experiments. The resulting isotherm shows the same general behavior, although a higher Kd of 20 mL/g was calculated for the linear part of the isotherm. The nonlinear part of the isotherm seems to begin at the same level of aqueous strontium concentration ($\sim 10^{-6}$ mol/L) and the

Table 4

Major cations concentrations in solution after 3 days for synthetic water/sand and deionized water/sand systems in batch reactors

Concentrations (mol/L)	K^+	Na^+	Ca^{2+}	Mg^{2+}	Sr^{2+}
Synthetic water in contact with sand	1.05×10^{-4}	6.5×10^{-5}	1.35×10^{-4}	1.9×10^{-5}	3×10^{-7}
Deionized water in contact with sand	7.9×10^{-5}	2.2×10^{-5}	6.2×10^{-5}	8×10^{-6}	1×10^{-6}

saturation level seems somewhat lower than the previous value obtained with "direct" batch experiments. A Langmuir model described the previous isotherm quite well with associated parameter values of 4.3×10^{-4} mol/kg for S_{max} and 4.73×10^{4} L/mol for K.

Chemical analyses show clearly that synthetic water is not in equilibrium with sand during initial contact. However, Na^{+} and Mg^{2+} concentrations seem to reach steady state after the five conditioning steps. A slight increase in K^{+} concentrations with conditioning seems to occur. The same is true for Ca^{2+} after a slight decrease observed during the first three washing steps. Global concentrations of competing cations (Ca^{2+}, Mg^{2+}) are lower than those measured in "direct" batch experiments, thus leading to an increasing Kd in the linear part of the isotherm in accordance with the cation exchange process. For the nonlinear part of the isotherm, an increase in concentration of the two main competing cations (Ca^{2+}, Mg^{2+}) are observed, this release being due to a competition effect caused by high stable strontium concentration. This general behavior is in good agreement with the theory of ion exchange which is assumed to control strontium sorption onto the studied sand.

These batch experiments indicated that Kd determination might be affected in the event of solid/solution disequilibria and the presence of significant amounts of stable strontium.

3.2. Stirred flow-through reactor studies

3.2.1. BTCs of conservative tracer

Eqs. (2) and (3) provided an excellent fit to measured BTCs of tritiated water over the entire range of flow rates tested. The presence of 8 g of sand in the reactor did not affect the tritiated water BTCs. Table 5 gives the fitted residence time (τ) of water in the reactor under different experimental conditions and shows the correlation factor used as a criterion for estimating the quality of the fit. It could be assumed that aqueous concentrations were homogeneous within the reactor and equal to that measured in the outflow.

3.2.2. Strontium sorption and transport

3.2.2.1. Kinetics and reversibility.   Strontium BTCs for $[Sr]_0 = 1.1 \times 10^{-6} \pm 0.05$ mol/L in synthetic groundwater at flow rates of 20, 100 and 200 mL/h are shown in Fig. 6. The BTCs are compared to the BTC of the inert tracer indicating retention of strontium on the sand. In the range of water residence times tested (between 10.3 and 103 min), the normalized total strontium BTCs were superimposed. In the experimental conditions of

Table 5
Comparison of water residence times (τ) in the stirred flow-through reactor determined by volumetric measurements of internal volume of the reactor and flow rate, and by fitting the parameter of the perfectly stirred reactor model on tritiated water BTCs

Flow rate (Q; mL/h)	Sand mass (g)	Stage II		Stage III		Volumetric measurements ($\tau = V_r/Q$; min)
		τ (min)	r^2	τ (min)	r^2	
100	0	20.5	0.99	20.1	0.99	20.4 ± 0.4
100	8	20.6	0.98	19.9	0.99	20.4 ± 0.4
20	8	102.8	0.98	101.1	0.98	102 ± 1.5
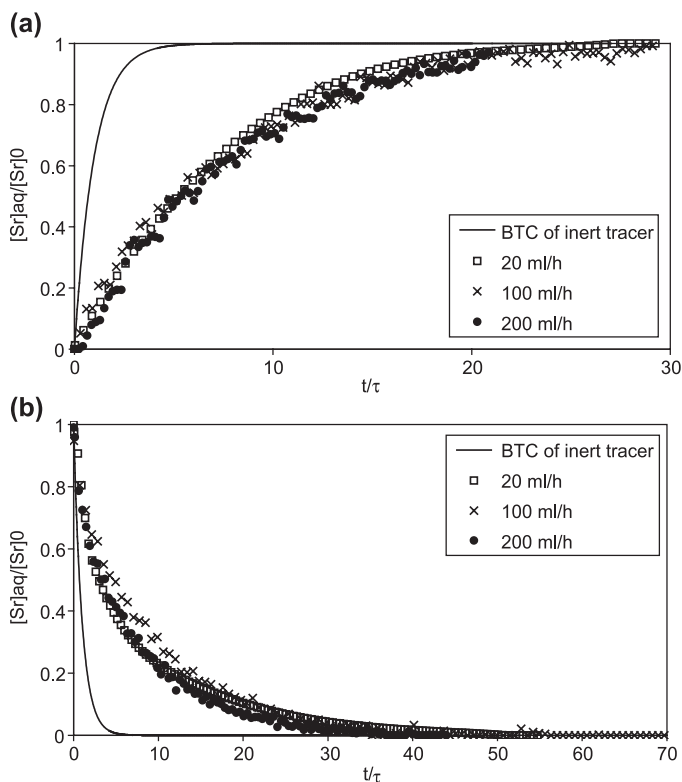
Fig. 6. Flow-through reactor BTCs of Sr for different flow rates (20 (□), 100 (x) and 200 (●) mL/h) compared to the BTC of the inert tracer (—). In this nondimensional representation (normalized strontium concentration as a function of normalized time), the BTCs of a nonreactive tracer are superimposed whatever the flow rate. $[Sr]_0$ was $1.1 \ 10^{-6}$ mol/L for all three experiments. (a) Stage II. (b) Stage III.

interest here, flow rate had no effect on the total strontium BTC. In other words, the characteristic time of the sorption mechanism observed under these experimental conditions is at least one order of magnitude less than 10.3 min, the shortest residence time tested for water in the reactor.

This upper value for characteristic fast sorption time must be borne in mind to determine the conditions under which kinetic treatment of sorption reaction is required to describe our column experiments. The Damkhöler number D_k (Saiers and Hornberger, 1996) can be calculated to check whether kinetics during the column experiment or natural groundwater flow rates are important. This dimensionless number relates the advection time scale to the kinetic adsorption time scale:

$$D_k = \frac{T_s}{T_{as}} \tag{13}$$

where T_{as} is the characteristic kinetic adsorption time. Jennings and Kirchner, (1984) reported that adsorption equilibrium could be assumed if $D_k > 100$. As the order of magnitude of T_{as} is 1 min, the characteristic advection time for the displacement

experiments must be approximately 100 mn for local equilibrium to be assumed. This analysis also indicates that the equilibrium approach may suffice on the field scale.

Another important result is that the strontium concentration in the outflow was within a few percent of the input concentration during stage II, even for the lowest flow rate and when the solution remained in contact with the sand for a long period (103 mn). Under these experimental conditions, there was no evidence of a "slow" sorption mechanism implying a continuous removal of dissolved strontium in the reactor.

The BTCs of strontium relating to the decreasing step could also be superimposed regardless of the flow rate between 20 and 200 mL/h. The quantity of sorbed strontium released during stage III was estimated and compared to the quantity sorbed during stage II. Results of desorption experiments showed that strontium removed from the solution by sorption was mostly reversibly bound to sand particles, with 80% to 100% of sorbed strontium recovered at the end of stage III depending on the length of the desorption stage (Table 2).

The amount of strontium released per reactor volume of synthetic water during stage III was also independent of the flow rate under the experimental conditions of this study. In the range of water residence times tested (10.3 to 103 mn), the desorption rate was slightly lower than the sorption rate (the maximum desorption rate was $75\pm5\%$ of the maximum sorption rate). Fig. 7 shows the evolution of sorption and desorption rates expressed as the amount in mol of strontium instantaneously removed from (stage II) or added to (stage III) the aqueous solution. However, this observation is consistent with the reversible and instantaneous cation exchange mechanism if the affinity of soil for Sr^{2+} is greater than for other major cations in solution. Further modeling (see Section 3.2.3) confirms this assumption.

3.2.2.2. Nonlinearity of sorption isotherm.   Fig. 8 represents the evolution of the normalized, total aqueous strontium concentration in the outflow as a function of the normalized time t/τ. BTCs were plotted at the same flow rate (100 mL/h), but with the
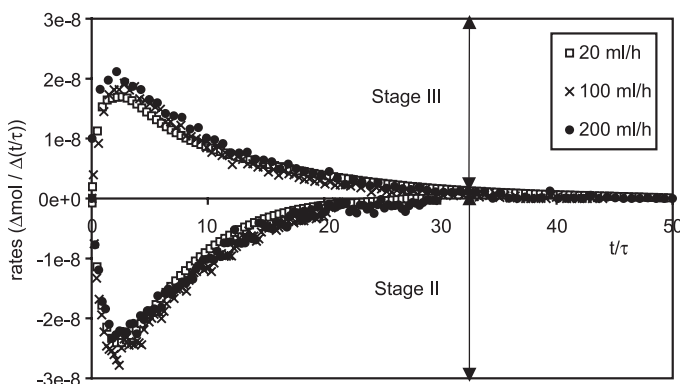
Fig. 7. Instantaneous Sr sorption rate (negative values) and desorption rate (positive values) calculated from the results of the stirred flow-through experiments at different flow rates and $[Sr]_0 = 1.1 \ 10^{-6}$ mol/L (see Fig. 6). Rates are expressed as the amount of aqueous strontium removed from (sorption stage) or added to (desorption stage) the solution for a given number of reactor volumes passing through the reactor.
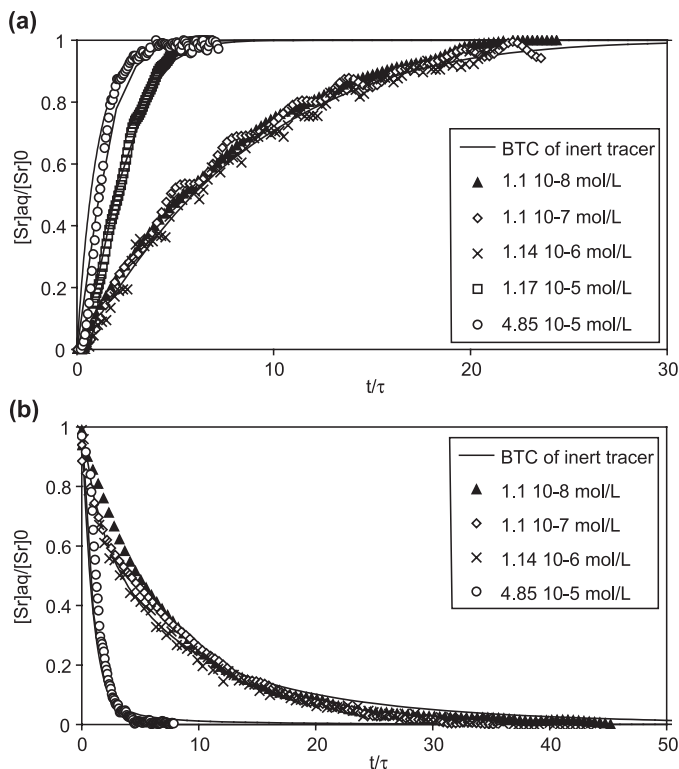
Fig. 8. Comparison of flow-through reactor BTCs of Sr for different inflow concentrations measured and predicted by the cation exchange model. Markers represent measured data while lines show fits obtained with PHREEQC (Section 3.2.3. for parameter values). Q was 100 mL/h for the five experiments. (a) Stage II. (b) Stage III.

input total aqueous concentration $[Sr]_0$ ranging from 4.85×10^{-5} mol/L to 1.1×10^{-8} mol/L. As soon as the outflow concentration was constant, the sand sample was assumed to be in equilibrium with the steady outlet solution and stage II was stopped. In the range of $[Sr]_0$ tested, steady-state dissolved strontium concentration always reached the same value as the input concentration.

The BTCs were compared to the BTC of the inert tracer indicating retention of strontium on the sand. The amount of strontium sorbed per unit mass of sand sample was in equilibrium with the total aqueous concentration of strontium reached at the end of stage II (the input concentration under these experimental conditions). The sorption isotherm of strontium on the eolian sand could then be plotted. Fig. 9 shows the strontium sorption isotherm determined by flow-through reactor technique in a more familiar representation and compares it to the isotherms obtained by batch techniques. The resulting adsorption isotherm data also fitted the Langmuir equation best, with the following values 5×10^{-5} mol/kg for S_{max} and $1.45 \ 10^6$ L/mol for K. The linear part of the isotherm finished at the same level as for batch experiments, but a higher Kd of 25 L/kg was obtained. Moreover, Fig. 9 shows that in batch experiments, the sorption capacity S_{max} of the sand for strontium
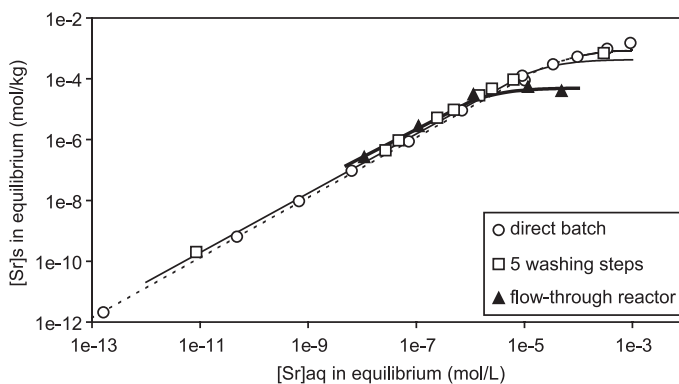
Fig. 9. Strontium sorption isotherms on the eolian sand and related fitted curves using the Langmuir model (($\bigcirc$) direct batch experiments, ($\square$) five washing steps and ($\blacktriangle$) flow-through reactor).

was one order of magnitude higher than in reactor experiments. Although similar results were obtained by Fesch et al. (1998), no clear reasons can be given yet to explain these discrepancies between batch and flow experiments.

The nonlinearity of sorption isotherms can be seen also clearly in Fig. 8. All the BTCs with input concentration $[Sr]_0 \leq 10^{-6}$ mol/L were superimposed in the nondimensional representation. In others words, in this range of total strontium aqueous concentration, the amount of sorbed strontium was independent of the steady (or equilibrium) strontium concentration in the liquid phase. The sorption isotherm was linear when the aqueous strontium concentration was less than 10^{-6} mol/L. When the input strontium concentration exceeded 10^{-6} mol/L, the difference in surface area between the nonreactive tracer BTC and the strontium BTC decreased. This means that the amount of sorbed strontium decreased, as did the slope of the sorption isotherm.

The same effect can be observed on the BTCs of strontium in response to the step decrease. Results of desorption experiments (Table 2) show that strontium removed from the solution by sorption was mostly reversibly bound to sand particles and that 80% to 100% of sorbed strontium was recovered at the end of stage III depending on the length of the desorption stage.

3.2.3. Modeling the nonlinear and reversible sorption process by cationic exchange

PHREEQC and the interaction model detailed in Section 2.6.1 were used to describe the BTCs of strontium resulting from the stirred flow-through reactor study. The two parameters of the model to be determined were the sorption capacity of the sand, X^- (mol/L) and the selectivity coefficient of Sr^{2+} with respect to Na^+. The value of the sorption capacity of the sand was already determined by using TableCurve to fit the Langmuir equation to the sorption isotherm resulting from the flow-through reactor study (Fig. 9).

The fitted parameter S_{max} in the Langmuir model is the sorption capacity of the sand for strontium, assuming that the stoichiometry of the sorption reaction: $Sr_{aq}+X=Sr-X$ is 1:1. One atom of the reactive element occupies one free sorption site X. The cation exchange reaction with the PHREEQC convention is written in the input file as: $Sr^{2+}+2X^-=SrX_2$. One free cation Sr^{2+} occupies two sites X^- to ensure the balance of charges. The number

of exchange sites X^- accessible for Sr^{2+} defined in the PHREEQC input file must be the S_{max} parameter of the Langmuir equation multiplied by 2 (the valence of the exchangeable cation) and converted to mol/L. As the mass of the sand sample (M) was 8 g and the volume of the solution (V_r) was 34 mL, this leads to the value: $X^- = 2\frac{M}{V_r}5 \times 10^{-5} = 2.35 \times 10^{-5}$ mol/L. Fig. 8 shows the results of fitting the selectivity coefficient of Sr^{2+} with respect to Na^+ to the Stage II results with PHREEQC. The value of the fitted parameter was: $\log K_{Sr/Na} = 2.6$.

The same model is used to describe the results obtained during stage III (Fig. 8). The partial irreversibility observed depends on the relative affinity of the soil surface for the cation in the inflow solution.

The interaction model built on the basis of the flow-through reactor study can be used to validate the assumption that the initial state of the sand sample was in equilibrium with the Sr-free synthetic water. Assuming that the sand without conditioning was in equilibrium with a solution containing 10^{-6} mol/L of strontium, as measured in the batch experiments (Table 4), the model can estimate the minimum number of reactor volumes needed to reach equilibrium with the Sr-free synthetic water during Stage I. Fig. 10 gives simulation results. A steady state in the outflow is reached after 50 reactor volumes have passed through. We are sure that under the flow-through reactor experimental conditions, the initial state of the sand was in equilibrium with the Sr-free synthetic water. In this case, the radioactive isotope of strontium was a tracer of the stable strontium. The sorption isotherm resulting from the measurement of the ^{85}Sr removal from the solution is representative of the total (stable and radioactive) strontium sorption isotherm. In the case of our batch experiments, even after five washing steps, the sand samples were not in equilibrium with the Sr-free synthetic groundwater and the initial amount of stable Sr sorbed onto the solid matrix was unknown. As the stable element concentrations are several orders of magnitude higher than the radioactive tracer concentration, the slope of the isotherm determined by the decrease in the volumetric activity of the solution between the initial state and equilibrium state can be underestimated if the isotherm is
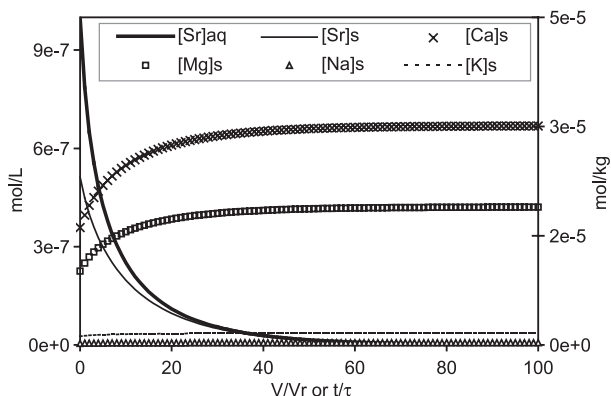
Fig. 10. Simulations with the cation exchange model of the evolution of $[Sr]_{aq}$, $[Sr]_s$, $[Ca]_s$, $[Mg]_s$, $[Na]_s$, and $[K]_s$ concentrations during Stage I. Note the different scales and units for the aqueous and sorbed concentration.

nonlinear. This phenomenon could explain the discrepancies observed between the Sr sorption isotherms obtained using the batch technique and the flow-through reactor technique, in particular, why the slope of the batch isotherm is smaller than that of the reactor isotherm for trace concentrations of total Sr.

This is the typical case on the Pilot Site. Analysis of the natural groundwater composition (Table 2) revealed that the average stable strontium concentration is 8.43×10^{-6} mol/L. This value is above the linearity limit of the real sorption isotherm of strontium (10^{-6} mol/L). According to the results of this study, the distance covered by the ^{90}Sr released from the trench since 1986 (10 m) can be explained by the nonlinearity of the Sr sorption isotherm.

3.3. Column studies

3.3.1. BTCs of inert tracer and hydrodynamic properties of the column

The hydrodynamic properties of the column packed with Pripyat eolian sand were inferred from the BTC of the nonreactive tracer: tritiated water. Typical normalized BTCs of tritium are included in Fig. 11. The BTCs measured at the beginning and at the end of the series of miscible displacement experiments were equal. After more than 5 months of operation and more than 1000 pore volumes of leaching, no change was observed in the hydrodynamic characteristics of the sand-packed column.

The BTCs were highly symmetric in shape. The data is well described by the one-dimensional advection–dispersion equation or AD model (Eq. (4)). The fitted value hydrodynamic dispersion coefficient is 0.56 cm^2/h. The hydraulic dispersivity of the sand-packed column (α=400 μm) is comparable to the grain size of the column matrix (d_{50}=225 μm). The fitted value of pore water velocity is 14.03 cm/h, the corresponding value of the Peclet number, $Pe=vL/D$ was 493 and the water residence time in the column was 1.4 h.
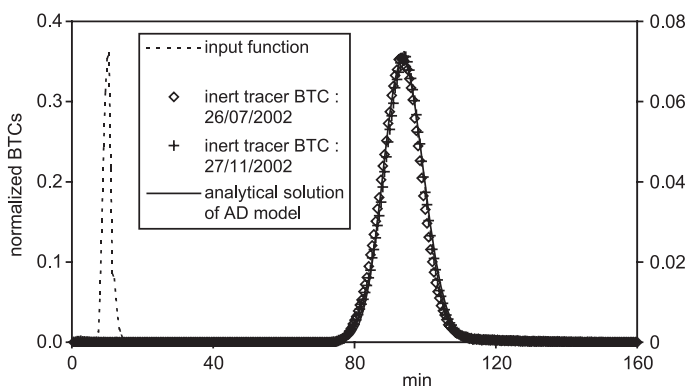
Fig. 11. Column BTCs of the inert tracer (tritiated water) at the start ($\diamond$; 07/2002) and end of the miscible displacement experiments (+; 11/2002). Markers represent measured data and continuous lines show the convolution product of the analytical solution of the advection–dispersion equation (—) in response to a Dirac input function with the measured input function (- - -).

From these observations, and the good agreement between the measured and predicted BTCs, it was concluded that uncertainty in physical transport parameters would not seriously complicate interpretations of reactive solute transport data.

3.3.2. Sorption and transport of reactive tracer

Table 3 gives the characteristics of the [85]Sr miscible displacement experiments performed in the sand packed column. Fig. 12 shows the [85]Sr breakthrough curves measured at four different stable strontium concentrations in the equilibrating solutions: Sr-free synthetic groundwater, synthetic groundwater with 9.5×10^{-7}, 2.5×10^{-6} and 8×10^{-6} mol/L of stable Sr. The curves are plotted as [85]Sr aqueous concentration vs. dimensionless time, represented as the number of pore volumes that has passed through the column. The difference in surface area under the curves is due to the difference in initial [85]Sr volumetric activity in the injected pulse. The surface area under the BTC (or zero order moment) is related to the amount of [85]Sr released from the column. For all experiments, the restitution level of [85]Sr reached 100%.

The [85]Sr retardation factor (Table 3) decreases as the stable strontium concentration in the equilibrating solution increases. This is clearly an effect of the nonlinearity of the Sr sorption isotherm. The [85]Sr BTCs were symmetrical despite the nonlinearity of the total Sr sorption isotherm because the [85]Sr aqueous concentration was several orders of magnitude lower than the stable Sr concentration and it induced only negligible variations in total Sr concentration. Therefore, the portion of total strontium sorption isotherm described is very small, and the slope does not change during the experiments.

From these observations, it was assumed that the [85]Sr sorption mechanism was fully reversible under these experimental conditions and the total Sr sorption isotherm was not linear. As the water residence time in the column, T_s was higher than the characteristic time of sorption resulting from flow-through reactor study (the Damköhler number D_k
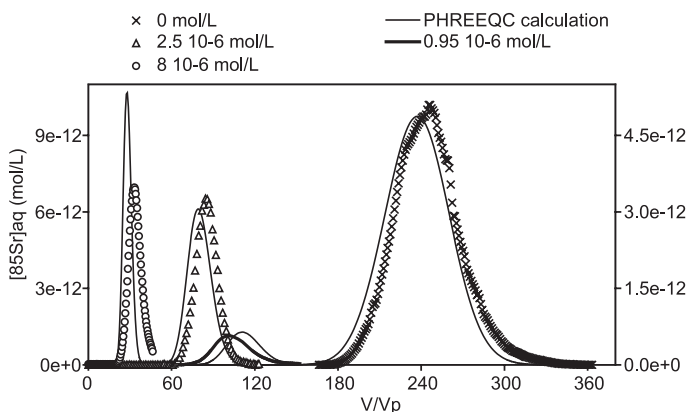
Fig. 12. Column BTCs of [85]Sr at different equilibrating stable Sr concentrations (see Table 3 for the isotopic ratio of the different solutions). Markers represent measured data and lines show PHREEQC simulations. Cation exchange model parameters were previously determined in independent flow-through reactor experiments and corrected only by the solid/liquid ratio, transport model parameters were fitted to the inert tracer BTC.

reached 84), we assumed that there was no kinetic sorption or desorption effects. The symmetry of the [85]Sr BTCs also confirms the assumption of chemical equilibrium (Schweich and Sardin, 1981).

As the results obtained in column experiments were consistent with the flow-through reactor study, it was decided to test the cation exchange model and use it to explain [85]Sr retardation factor variations as a function of stable strontium concentration. It was then necessary to add the new [85]Sr species to the PHREEQC database. No parameter fitting was performed at this step. Transport parameters were already determined with the nonreactive tracer BTC analysis and were directly imported into the PHREEQC input file. All the selectivity constants of major cations with respect to Na^+ were conserved. The selectivity constant of the new species [85]Sr^{2+} with respect to Na^+ was equal to that of stable Sr^{2+} with respect to Na^+ (log $K_{Sr/Na}$=2.6). The number of exchange sites accessible for Sr^{2+} in our physicochemical conditions resulting from the flow-through reactor study was used: X^-=10^{-4} mol/kg. In order to allow for the increase in solid/liquid ratio between the flow-through reactor and column, the number of exchange sites was calculated as 10^{-4} M/V, where M is the solid mass per unit of porous medium volume and V is the water volume per unit of porous medium volume. The resulting number of exchange sites accessible for Sr^{2+} in our experimental conditions, X^-, in mol per unit volume of water in the porous media was $10^{-4}\rho_d/\theta_{sat}$=$5\times10^{-4}$ mol/L.

Considering that the sand without conditioning was in equilibrium with a solution containing 10^{-6} mol/L of strontium, as measured in batch experiments (Table 4) and taking into account the conditioning stage length in the PHREEQC simulations of each column experiment (Table 3), it was then possible to describe the [85]Sr BTCs. The theoretical BTCs obtained from PHREEQC calculations for the different [85]Sr miscible displacement experiments were compared with the experimental BTCs on Fig. 12. There was good agreement between the measured and predicted [85]Sr BTCs when the length of the equilibrating stage was included in the transport calculations. The retardation factor and maximum aqueous concentration were well estimated.

4. Discussion and conclusions

In this work, we have examined the effects of nonlinear sorption and competition with stable strontium on radioactive [85]Sr transport in a natural sand. Using a multiple tracer approach, different physical and chemical processes (including hydrodynamic transport, nonlinear sorption, and competition with major cations) were identified and quantified. Batch, reactor and miscible displacement experiments were performed covering a wide range of experimental conditions.

Experiments under dynamic conditions, namely flow-through reactor and column experiments, were in very good agreement. However, the solid/liquid ratio was very different (0.24 g/mL for the reactor and 5.0 g/mL for the sand-packed column). Sand particles in the reactor were dispersed and shaken, whereas the sand sample was packed in the column. The experimental data resulting from the flow-through reactor study showed evidence of a nonlinear sorption process. The results were modeled with the PHREEQC computer code (Version 2). A cation exchange model proved suitable for describing the

solute/soil reaction. Two parameters were fitted: the number of exchange sites accessible for Sr^{2+} and the selectivity constant of Sr^{2+} with respect to Na^+. This model successfully described the results of the entire set of miscible displacement experiments using the same set of parameter values for reaction calculations. Miscible displacement experiments were conducted to demonstrate competition between stable and radioactive strontium and its effect on the ^{85}Sr retardation factor. This study was performed for two reasons: the nonlinearity of the Sr sorption isotherm for the eolian sand and the highly stable strontium aqueous concentration levels observed in the field.

Based on these observations, explanations can be proposed for the discrepancies found between data obtained from static (batches) and dynamic (reactor and column) experiments. The adsorption isotherm data obtained from the batch study also fitted the Langmuir isotherm best. In batch experiments, however, the sorption capacity of the sand for radioactive strontium was one order of magnitude higher than in dynamic experiments and the slope of the isotherm was lower. Neither the "solid/solution ratio effect", nor the increase in accessible reactive surface area resulting from the disaggregation of clay clusters during shaking and/or from abrasion processes can be put forward, for if such effects had existed, they would have led to discrepancies between flow-through reactor and column results. Classical alternative explanations include a loss of fine particles (with higher reactivity) during the initial conditioning of the sand sample in the reactor (that hardly occurs in the column) or an inadequate control of solution and exchanger composition during the equilibrium period in the batch system (Porro et al., 2000). Desorbed antecedent species (stable Sr for example) are removed from the column or reactor in the flow system but remain to compete for sorption sites in the batch system. This will affect exchange equilibria in batch systems, but not in flow systems, because the exchanger is in equilibrium with the feed solution thanks to the conditioning stage and because the solution-phase composition is relatively constant.

Static and dynamic experiments provide two different sets of parameters for the cation exchange model. We have shown the influence of the conditioning of the soil on the values of the fitted parameters, especially the number of exchange sites accessible for Sr^{2+}. The geochemistry of the soil/solution system has to be controlled accurately during experiments because small variations of the concentration and nature of competitive cations in solution has a large influence on the fitted number of exchange sites accessible for Sr^{2+} due to the nature of the sand. Static and dynamic experiments provide a range of values for the parameters of the cation exchange model. However, we can say that, in flow systems, the number of unknown variables decreases and the fitting of the model parameters is facilitated.

We have shown that an increase of the stable Sr concentration in water from 10^{-6} to 10^{-5} mol/L leads to divide the radioactive Sr retardation factor by 3. Knowing the spatial and temporal variability of stable Sr concentration in groundwater at the field scale, it seems not realistic to use a single Kd value to predict the ^{90}Sr migration in aquifer. Maturation of the organic matter content of the trench could lead to future perturbations of the geochemistry of the system, especially Ca^{2+} concentration and pH. These two variables have also an effect on the retardation factor of Sr and additional studies are planned to quantify this effect in terms of range of Kd values.

Acknowledgements

References

Albrecht, A., Schultze, U., Bello Bugallo, P., Wydler, H., Frossard, E., Flühler, H., 2003. Behavior of surface applied radionuclide and a dye tracer in structured and repacked monoliths. J. Environ. Radioact. 68, 47–64.

Appelo, C.A.J., Verweij, E., Schäfer, H., 1998. A hydrogeochemical transport model for an oxidation experiment with pyrite/calcite/exchangers/organic matter containing sand. Appl. Geochem. 13, 257–268.

Bajracharya, K., Tran, Y.T., Barry, D.A., 1996. Cadmium adsorption at different pore water velocities. Geoderma 73, 197–216.

Bolt, G.H., Bruggenwert, M.G.M. (Eds.), 1978. Soil Chemistry: A. Basic Elements. Elsevier, Amsterdam. 527 pp.

Bolz, R.E., Tuve, G.L., 1976. CRC Handbook of tables for Applied Engineering Science. (2nd edition)CRC Press, Boca Raton (USA). 1166 pp.

Bruggenwert, M.G.M., Kamphorst, A., 1982. Survey of experimental information on cation exchange in soil systems. In: Bolt, G.H. (Ed.), Soil Chemistry: B. Physico-Chemical Models. Elsevier, Amsterdam, pp. 141–203.

Brusseau, M.L., 1994. Transport of reactive contaminants in heterogeneous porous media. Rev. Geophys. 32, 285–313.

Bugaï, D.A., Guillou, Ph., Dewiere, L., Dzhepo, S.P., Gerbaux, O., Getto, D., et al., 2000. Study of radionuclide migration in geological environment at experimental polygon pilot site in the area of the near-surface disposal of radioactive wastes in the near-zone of chernobyl NPP. In: Shestopalov, V. (Eds.), Water Exchange and Chernobyl Accident, Distribution of Chernobyl Radionuclides in Hydrogeology Structures, vol. 1. Ukrainian National Academy of Sciences, Kiev, pp. 346–383. (In Russian).

Bugaï, D., Dewiere, L., Kashparov, V.A., Ahamdach, N., 2002. Strontium-90 transport parameters from source term to aquifer in the chernobyl pilot site. Radioprotection-Colloques 37-C1, 11–16.

Dewiere, L., Bugaï, D., Grenier, C., Kashparov, V., Ahamdach, N., 2004. [90]Sr migration to the geosphere from a waste burial in the chernobyl exclusion zone. J. Environ. Radioact. 74, 139–150.

Fesch, C., Simon, W., Haderlein, S.B., Reichert, P., Schwarzenbach, R.P., 1998. Nonlinear sorption and nonequilibrium solute transport in aggregated porous media: experiments, process identification and modeling. J. Contam. Hydrol. 33, 373–407.

Gabriel, U., Gaudet, J.P., Spadini, L., Charlet, L., 1998. Reactive transport of uranyl in a goethite column: an experimental and modelling study. Chem. Geol. 151, 107–128.

Grolimund, D., Borkovec, M., Federer, P., Sticher, H., 1995. Measurement of sorption isotherms with flow-through reactors. Environ. Sci. Technol. 29, 2321–2371.

Hilton, J., Nolan, L., Jarvis, K.E., 1997. Concentrations of stable isotopes of cesium and strontium in freshwaters in northern England and their effect on estimates of sorption coefficients (Kd). Geochim. Cosmochim. Acta 61 (6), 1115–1330.

Hormann, V., Kirchner, G., 2002. Prediction of the effects of soil-based countermeasures on soil solution chemistry of soils contaminated with radiocesium using the hydrogeochemical code PHREEQC. Sci. Total Environ. 289, 83–95.

Jackson, R.F., Inch, J., 1983. Hydrogeochemical processes affecting the migration of radionuclides in a fluvial and aquifer at the chalk river nuclear laboratories. Environ. Sci. Technol. 17, 231.

Jennings, A.A., Kirchner, D.J., 1984. Instantaneous equilibrium approximation analysis. J. Hydraul. Eng., Proc. Am. Soc. Civ. Eng. 11, 1700–1717.

Jury, W.A., Sposito, G., 1985. Field calibration and validation of solute transport models for the unsaturated zone. Soil Sci. Soc. Am. J. 49, 1331–1341.

Jury, W.A., Roth, K., 1990. Transfer Functions and Solute Movement Through Soil: Theory and Applications. Birkhäuser, Basel, Switzerland.

Keren, R., O'Connor, G.A., 1983. Strontium adsorption by noncalcareous soils–exchangeable ions and solution composition effects. Soil Sci. 135 (5), 308–315.

Kinniburgh, D.G., Syers, J.K., Jackson, M.L., 1975. Specific adsorption of trace amount of calcium and strontium by hydrous oxides of iron and aluminium. Proc.-Soil Sci. Soc. Am. 39, 464–470.

Koss, V., Kim, J.I., 1990. Modeling of strontium sorption and speciation in a natural sediment—groundwater system. J. Contam. Hydrol. 6, 267–280.

Lefevre, F., Sardin, M., Schweich, D., 1993a. Migration of strontium in clayey and calcareous sandy soil: precipitation and ion exchange. J. Contam. Hydrol. 13, 215–229.

Lefevre, F., Sardin, M., Vitorge, P., 1993b. Migration of ^{45}Ca ^{90}Sr in a clayey and calcareous sand: calculation of distribution coefficients. 4th International Conference on the Chemistry and Migration Behaviour of Actinides and Fission Products in the Geosphere, Charleston, SC USA, December 12–17 1993, pp. 711–717.

Martin-Garin, A., van Capellen, P., Charlet, L., 2003. Aqueous cadmium uptake by calcite: a stirred flow-through reactor study. Geochim. Cosmochim. Acta 67 (15), 2763–2774.

Metson, A.J., 1956. Methods of chemical analysis for soil survey samples. N.Z. Soil Bur., 12.

Ohnuki, T., 1994. Sorption characteristics of strontium on sandy soils and their components. Radiochim. Acta 64, 237–245.

Pang, L., Close, M., 1999. Field-scale physical non-equilibrium transport in an alluvial gravel aquifer. J. Contam. Hydrol. 38, 447–464.

Parkhurst, D.L., Appelo, C.A.J., 1999. User's guide to PHREEQC (Version 2)—a computer program for speciation, batch-reaction, one-dimensional transport, and inverse geochemical calculations, U.S.G.S. Water-Resources Report 99-4259.

Plassard, F., Winiarski, T., Petit-Ramel, M., 2000. Retention and distribution of three heavy metals in a carbonated soil: comparison between batch and unsaturated column studies. J. Contam. Hydrol. 42, 99–111.

Porro, I., Newman, M.E., Dunnivant, F.M., 2000. Comparison of batch and column methods for determining strontium distribution coefficient for unsaturated transport in basalt. Environ. Sci. Technol. 34, 1679–1686.

Prommer, H., Davis, G.B., Barry, D.A., 1999. Geochemical changes during biodegradation of petroleum hydrocarbons: field investigations and biogeochemical modelling. Org. Geochem. 30, 423–435.

Prout, W.E., 1958. Adsorption of radioactive wastes by Savannah river plant soil. Soil Sci. 86, 13–17.

Saiers, J.E., Hornberger, G.M., 1996. Migration of ^{137}Cs through quartz sand: experimental results and modeling approaches. J. Contam. Hydrol. 22, 255–270.

Sardin, M., Schweich, D., Leij, F.J., Van Genuchten, M.T., 1991. Modeling the nonequilibrium transport of linearly interacting solutes in porous media: a review. Water Resour. Res. 27, 2287–2307.

Schoen, R., Gaudet, J.P., Bariac, T., 1999. Preferential flow and solute transport in a large lysimeter, under controlled boundary conditions. J. Hydrol. 215, 70–81.

Schweich, D., Sardin, M., 1981. Adsorption, partition, ion exchange and chemical reaction in batch reactors or in column—a review. J. Hydrol. 50, 1–33.

Šimůnek, J., Jarvis, N.J., van Genuchten, M.Th., Gärdenäs, A., 2003. Review and comparison of models for describing non-equilibrium and preferential flow and transport in the Vadose Zone. J. Hydrol. 272, 14–35.

Thomasson, M.J., Wierenga, P.J., 2003. Spatial variability of the effective retardation factor in the unsaturated field soil. J. Hydrol. 272, 213–225.

Tran, Y.T., Barry, D.A., Bajracharya, K., 2002. Cadmium desorption in sand. Environ. Int. 28, 493–502.

van Breukelen, B.M., Appelo, C.A.J., Olsthoorn, T.N., 1998. Hydrogeochemical transport modelling of 24 years of Rhine water infiltration in the dunes of the Amsterdam water supply. J. Hydrol. 209, 281–296.

van Capellen, P., Qiu, L., 1997a. Biogenic silica dissolution in sediments of the southern ocean: I. Solubility. Deep-Sea Res., II 44, 1109–1128.

van Capellen, P., Qiu, L., 1997b. Biogenic silica dissolution in sediments of the southern ocean: II. Kinetics. Deep-Sea Res., II 44, 1129–1149.

Villermaux, J., 1985. Génie de la réaction chimique: conception et fonctionnement des réacteurs. Lavoisier Tec-Doc, Paris. (In French).

Wen, C.Y., Fan, L.T., 1975. Models for Flow Systems and Chemical Reactors. Dekker M., New York.